Chinese Journal of Physiology 56(1): 26-35, 2013
DOI: 10.4077/CJP.2013.BAA091

M-3M3FBS-Induced Ca^{2+} Movement and Apoptosis in HA59T Human Hepatoma Cells

Shiuh-Inn Liu[1], Ko-Long Lin[2], Ti Lu[3], Yi-Chau Lu[4], Shu-Shong Hsu[1], Jeng-Yu Tsai[1], Wei-Chuan Liao[1], Fong-Dee Huang[1], Chao-Chuan Chi[5], Wei-Zhe Liang[6], Li-Ling Tseng[7], An-Jen Chiang[8], and Chung-Ren Jan[9]

[1]*Department of Surgery, Kaohsiung Veterans General Hospital, Kaohsiung 81362*
[2]*Department of Rehabilitation, Kaohsiung Veterans General Hospital, Kaohsiung 81362*
[3]*Department of Psychiatry, Kaohsiung Veterans General Hospital, Kaohsiung 81362*
[4]*Department of Orthopedics, Kaohsiung Veterans General Hospital, Kaohsiung 81362*
[5]*Department of Otolaryngology, Kaohsiung Veterans General Hospital, Kaohsiung 81362*
[6]*Department of Biological Sciences, National Sun Yat-Sen University, Kaohsiung 80424*
[7]*Department of Dentistry, Kaohsiung Veterans General Hospital, Kaohsiung 81302*
[8]*Department of Obstetrics and Gynecology, Kaohsiung Veterans General Hospital, Kaohsiung 81362*
and
[9]*Department of Medical Education and Research, Kaohsiung Veterans General Hospital Kaohsiung 81362, Taiwan, Republic of China*

Abstract

The effect of 2,4,6-trimethyl-N-(meta-3-trifluoromethyl-phenyl)-benzenesulfonamide (*m*-3M3FBS), a presumed phospholipase C activator, on cytosolic free Ca^{2+} concentrations ($[Ca^{2+}]_i$) in HA59T human hepatoma cells is unclear. This study explored whether *m*-3M3FBS elevated basal $[Ca^{2+}]_i$ levels in suspended cells by using fura-2 as a Ca^{2+}-sensitive fluorescent dye. *M*-3M3FBS at concentrations of 10-50 μM increased $[Ca^{2+}]_i$ in a concentration-dependent fashion. The Ca^{2+} signal was reduced partly by removing extracellular Ca^{2+}. *M*-3M3FBS-induced Ca^{2+} influx was inhibited by nifedipine, econazole, SK&F96365, aristolochic acid, and GF109203X. In Ca^{2+}-free medium, 50 μM *m*-3M3FBS pretreatment inhibited the $[Ca^{2+}]_i$ rise induced by the endoplasmic reticulum Ca^{2+} pump inhibitor thapsigargin. Conversely, pretreatment with thapsigargin partly reduced *m*-3M3FBS-induced $[Ca^{2+}]_i$ rise. Inhibition of inositol 1,4,5-trisphosphate formation with U73122 did not alter *m*-3M3FBS-induced $[Ca^{2+}]_i$ rise. At concentrations between 10 and 40 μM *m*-3M3FBS killed cells in a concentration-dependent manner. The cytotoxic effect of *m*-3M3FBS was not reversed by prechelating cytosolic Ca^{2+} with 1,2-bis(2-aminophenoxy)ethane-N,N,N',N'-tetraacetic acid (BAPTA). Annexin V/propidium iodide staining data suggest that *m*-3M3FBS induced apoptosis in a concentration-dependent manner. *M*-3M3FBS also increased levels of reactive oxygen species. Together, in human hepatoma cells, *m*-3M3FBS induced a $[Ca^{2+}]_i$ rise by inducing phospholipase C-independent Ca^{2+} release from the endoplasmic reticulum and Ca^{2+} entry *via* protein kinase C-sensitive store-operated Ca^{2+} channels. *M*-3M3FBS induced cell death that might involve apoptosis *via* mitochondrial pathways.

Key Words: Ca^{2+}, *m*-3M3FBS, hepatoma, apoptosis

Introduction

2,4,6-Trimethyl-N-(meta-3-trifluoromethyl-phenyl)-benzenesulfonamide (*m*-3M3FBS) was originally shown to induce a transient rise in cytosolic Ca^{2+} concentration ($[Ca^{2+}]_i$) in neutrophils *via* activation

Corresponding author: Dr. Chung-Ren Jan, Department of Medical Education and Research, Kaohsiung Veterans General Hospital, Kaohsiung 81362, Taiwan, R.O.C. Tel: +886-7-3422121 ext. 1509, Fax: +886-7-3468056, E-mail: crjan@isca.vghks.gov.tw
Received: December 21, 2011; Revised: March 7, 2012; Accepted: March 13, 2012.
 ISSN : 0304-4920. http://www.cps.org.tw

of phospholipase C (PLC) (1). Based on this finding, *m*-3M3FBS was used as a selective PLC activator in different cell types such as neurons (24), membrane (11), submandibular gland cells (17), B lymphocytes (25), epithelial cells (28), and taste cells (10). These studies all interpret their results assuming that *m*-3M3FBS completely inhibited PLC without other unexpected effects. Not surprisingly, contradictory evidence from SH-SY5Y human neuroblastoma cells suggested that *m*-3M3FBS changed Ca^{2+} movement without activation of PLC (21). Therefore, the exact molecular mechanisms of *m*-3M3FBS are unclear.

A change in $[Ca^{2+}]_i$ is a key message for diverse biological responses in nearly all cells (4). Thus, a unregulated $[Ca^{2+}]_i$ signal often leads to abnormality of ion movement, dysfunction of enzymes, apoptosis, necrosis, and proliferation, *etc* (9). In human renal Caki cancer cells, *m*-3M3FBS was suggested to cause apoptosis *via* inducing a $[Ca^{2+}]_i$ rise; however, how this Ca^{2+} signal arose was unexplored (20). *M*-3M3FBS was found to release Ca^{2+} from internal stores in rat primary cortical neuronal cells and pheochromocytoma (PC12) cells (19) without elucidating the mechanism. In contrast, in MDCK renal cells and PC3 prostate cancer cells, it has been reported that *m*-3M3FBS induced a $[Ca^{2+}]_i$ rise by releasing Ca^{2+} and causing store-operated Ca^{2+} entry in a PLC-independent manner (13). However, whether this Ca^{2+} signal leads to changes in cell viability or apoptosis was unknown.

The aim of the present study was to further investigate this question by measuring effect of *m*-3M3FBS on $[Ca^{2+}]_i$, viability, cell cycle, apoptosis, and reactive oxygen species (ROS) production by using HA59T human hepatoma cells. This cell line is a useful model for human hepatoma research. It has been shown that in this cell, robust $[Ca^{2+}]_i$ rises can be observed by stimulation with several agents including diindolylmethane (8), carvedilol (7) and calmidazolium (23). Fura-2 was used as a fluorescent Ca^{2+}-sensitive dye to measure $[Ca^{2+}]_i$ changes. The effect of *m*-3M3FBS on $[Ca^{2+}]_i$ rises both in the presence and absence of extracellular Ca^{2+}, the concentration-response plot, the pathways underlying Ca^{2+} entry and Ca^{2+} release, the internal Ca^{2+} stores, and the role of PLC were explored. Moreover, the effect of *m*-3M3FBS on viability, cell cycle, apoptosis, and production of ROS are explored.

Materials and Methods

Materials

The reagents for cell culture were from Gibco (Gaithersburg, MD, USA). Other reagents were from Sigma-Aldrich (St. Louis, MO, USA).

Cell Culture

HA59T human hepatoma cells purchased from Bioresource Collection and Research Center (Taiwan) were cultured in Dulbecco's modified Eagle medium supplemented with 10% heat-inactivated fetal bovine serum, 100 U/ml penicillin and 100 µg/ml streptomycin.

Solutions Used in $[Ca^{2+}]_i$ Measurements

Ca^{2+}-containing medium (pH 7.4) contained 140 mM NaCl, 5 mM KCl, 1 mM $MgCl_2$, 2 mM $CaCl_2$, 10 mM Hepes, and 5 mM glucose. *M*-3M3FBS was dissolved in dimethyl sulfoxide as a 1 M stock solution. The other agents were dissolved in water, ethanol or dimethyl sulfoxide. The concentration of organic solvents in the solution used in experiments did not exceed 0.1%, and did not alter viability or basal $[Ca^{2+}]_i$.

$[Ca^{2+}]_i$ Measurements

Confluent cells grown on 6 cm dishes were trypsinized and made into a suspension in culture medium at a density of 10^6 cells/ml. Cells were subsequently loaded with 2 µM fura-2/AM for 30 min at 25°C in the same medium. After loading, cells were washed with Ca^{2+}-containing medium twice and were resuspended in Ca^{2+}-containing medium at a density of 10^7 cells/ml. Fura-2 fluorescence measurements were performed in a water-jacketed cuvette (25°C) with continuous stirring; the cuvette contained 1 ml of medium and 0.5 million cells. Fluorescence was monitored with a Shimadzu RF-5301PC spectrofluorophotometer immediately after 0.1 ml cell suspension was added to 0.9 ml Ca^{2+}-containing or Ca^{2+}-free medium, by recording excitation signals at 340 nm and 380 nm and emission signal at 510 nm at 1-sec intervals. During the recording, reagents were added to the cuvette by pausing the recording for 2 sec to open and close the cuvette-containing chamber. For calibration of $[Ca^{2+}]_i$, after completion of the experiments, the detergent Triton X-100 and 5 mM $CaCl_2$ were added to the cuvette to obtain the maximal fura-2 fluorescence. Then the Ca^{2+} chelator EGTA (10 mM) was subsequently added to chelate Ca^{2+} in the cuvette to obtain the minimum fura-2 fluorescence. $[Ca^{2+}]_i$ was calculated as previously described (6, 12, 16, 32).

Cell Viability Assays

The measurement of cell viability was based on the ability of cells to cleave tetrazolium salts by dehydrogenases. Augmentation in the amount of developed color directly correlated with the number of live cells. Assays were performed according to

manufacturer's instructions designed specifically for this assay (Roche Molecular Biochemical, Indianapolis, IN, USA). Cells were seeded in 96-well plates at a density of 10,000 cells/well in culture medium for 24 h in the presence of 0-40 μM *m*-3M3FBS. The cell viability detecting reagent 4-[3-[4-Iodophenyl]-2-4(4-nitrophenyl)-2H-5-tetrazolio-1, 3-benzene disulfonate] (WST-1; 10 μM pure solution) was added to samples after *m*-3M3FBS treatment, and cells were incubated for 30 min in a humidified atmosphere. In experiments using BAPTA/AM to chelate cytosolic Ca^{2+}, fura-2-loaded cells were treated with 10 μM BAPTA/AM for 1 h prior to incubation with *m*-3M3FBS. The cells were washed once with Ca^{2+}-containing medium and incubated with or without *m*-3M3FBS for 24 h. The absorbance of samples (A_{450}) was determined using enzyme-linked immunosorbent assay (ELISA) reader. Absolute optical density was normalized to the absorbance of unstimulated cells in each plate and expressed as a percentage of the control value.

Alexa ®Flour 488 Annexin V/Propidium Iodide (PI) Staining for Apoptosis

Annexin V/PI staining assay was employed to further detect cells in early apoptotic and late apoptotic/necrotic stages. Cells were exposed to *m*-3M3FBS at concentrations of 0, 20 μM, or 40 μM for 24 h. Cells were harvested after incubation and washed in cold phosphate-buffered saline (PBS). Cells were resuspended in 400 μl reaction solution with 10 mM of HEPES, 140 mM of NaC1, 2.5 mM of $CaC1_2$ (pH 7.4). Alexa Fluor 488 annexin V/PI staining solution (Probes Invitrogen, Eugene, OR, USA) was added in the dark. After incubation for 15 min, the cells were collected and analyzed in a FACScan flow cytometry analyzer. Excitation wavelength was at 488 nm and the emitted green fluorescence of Annexin V (FL1) and red fluorescence of PI (FL2) were collected using 530 nm and 575 nm band pass filters, respectively. A total of 20,000 cells were analyzed per sample. Light scatter was measured on a linear scale of 1024 channels and fluorescence intensity was on a logarithmic scale. The amount of early apoptosis and late apoptosis/necrosis were determined, respectively, as the percentage of Annexin V^+/PI^- or Annexin V^+/PI^+ cells. Data were later analyzed using the flow cytometry analysis software WinMDI 2.8 (by Joe Trotter, freely distributed software). X and Y coordinates refer to the intensity of fluorescence of Annexin and PI, respectively.

PI Staining of Cellular DNA

Adherent and floating cells were pooled, washed with PBS, then fixed in PBS-methanol (1:2) solution and, finally, maintained at 4°C for 18 h. Following two more washes with PBS, the cell pellet was stained with the fluorescent probe solution containing PBS, 40 μg PI /ml and 40 μg DNase-free RNaseA/ml for 30 min at room temperature in the dark. Cells were then analyzed using a FACScan flow cytometer with excitation at 488 nm, with gating out of doublets and clumps using pulse processing and collection of fluorescence emission above 620 nm. The percentage of cells undergoing DNA damage was obtained from the percentage of cells in the distinct subdiploid region of the DNA distribution histograms.

Detection of Intracellular Reactive Oxygen Species (ROS) by Flow Cytometry

Cells were plated in triplicate at a density of 2×10^5 cells/well in 6-well plates (Falcon, BD Biosciences, Franklin Lakes, NJ, USA). After overnight incubation, cells were treated with several concentrations of *m*-3M3FBS for 24 h. Cells were harvested, washed twice with cold PBS, and then 2',7'-dichlorofluorescein diacetate (DCFH-DA) and dihydroethidine (DHE) were added at a final concentration of 50 μg/ml in Ca^{2+}-containing medium. Cells were incubated for 30 min at 37°C. After cells were washed twice with cold PBS, 1 ml cold PBS was added. These two fluorescent probes were commonly used for detection of intracellular oxidants. During an intracellular oxidative burst, ROS are usually generated, leading to the conversion of the non-fluorescent probes into fluorescent molecules. The oxidation product of DCFH is dichloroflurescein (DCF), with the green emission at 529 nm, while that of DHE is ethidium, emitting red fluorescence at 590 nm with a FACS Calibur flow cytometer (BD Biosciences, Franklin Lakes, NJ, USA). Data were later analyzed using the flow cytometry analysis software WinMDI 2.8 (by Joe Trotter, freely distributed software) by gating 10^2-10^4 areas of the X and Y coordinates.

Statistics

Data are reported as means ± SEM of 3-5 experiments. Data were analyzed by two-way analysis of variances (ANOVA) using the Statistical Analysis System (SAS®, SAS Institute Inc., Cary, NC, USA). Multiple comparisons between group means were performed by *post-hoc* analysis using the Tukey's HSD (honestly significantly difference) procedure. A *P*-value less than 0.05 is considered significant.

Results

Fig. 1A shows that the basal $[Ca^{2+}]_i$ level was

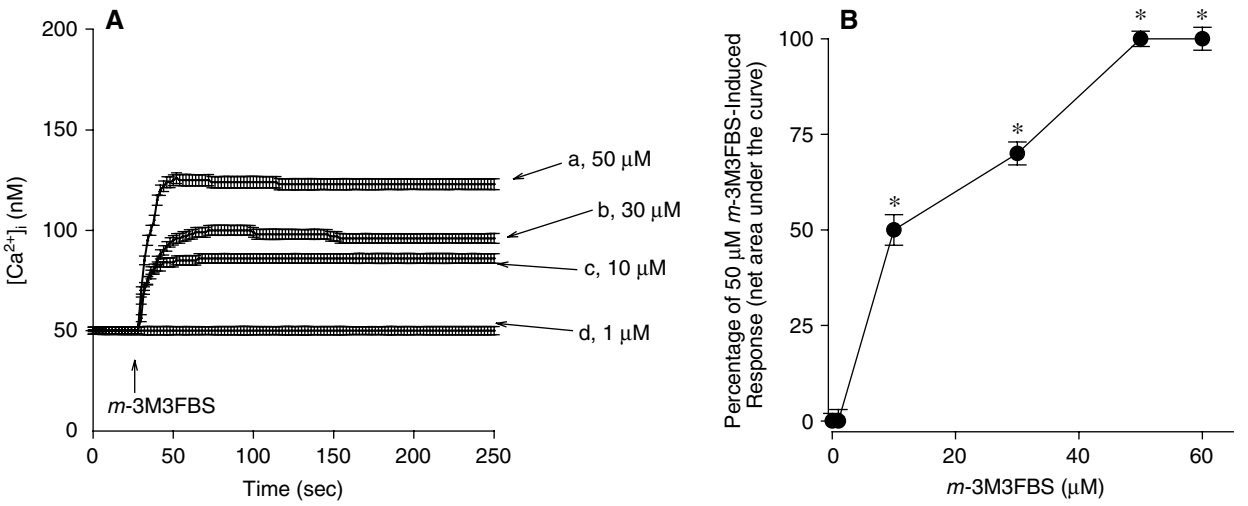

Fig. 1. (A) Effect of *m*-3M3FBS on $[Ca^{2+}]_i$ in fura-2-loaded HA59T cells. *M*-3M3FBS was added at 25 sec. The concentration of *m*-3M3FBS was indicated. The experiments were performed in Ca^{2+}-containing medium. (B) A concentration-response plot of *m*-3M3FBS-induced Ca^{2+} signals. Y axis is the percentage of control which is the net (baseline subtracted) area under the curve (25-250 sec) of the $[Ca^{2+}]_i$ rise induced by 50 μM *m*-3M3FBS. Data are means ± SEM of three experiments. $*P < 0.05$ compared to control.

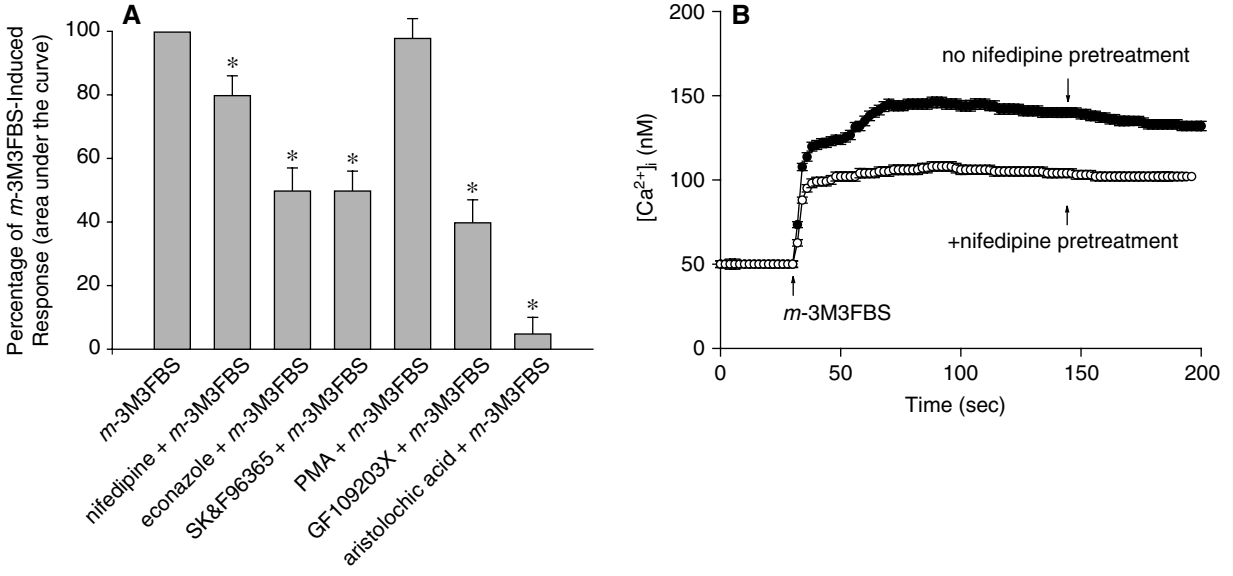

Fig. 2. Effect of Ca^{2+} channel blockers and phospholipase A_2 inhibitor on *m*-3M3FBS-induced $[Ca^{2+}]_i$ rise. The experiments were performed in Ca^{2+}-containing medium. The $[Ca^{2+}]_i$ rise induced by 50 μM *m*-3M3FBS was taken as control. (A) In blocker- or modulator-treated groups, the reagent was added 1 min before *m*-3M3FBS. The concentration was 1 μM for nifedipine, 0.5 μM for econazole, 1 μM for SK&F96365; 20 μM for aristolochic acid, 10 nM for phorbol 12-myristate 13-acetate (PMA) and 2 μM for GF109203X. Data are expressed as the percentage of control (1st column) that is the maximum value of 50 μM *m*-3M3FBS-induced $[Ca^{2+}]_i$ rise, and are means ± SEM of three experiments. $*P < 0.05$ compared to control. (B) Recordings of *m*-3M3FBS-induced $[Ca^{2+}]_i$ rises in the absence and presence of nifedipine.

50 ± 2 nM. At concentrations between 10 and 50 μM, *m*-3M3FBS evoked $[Ca^{2+}]_i$ rises in a concentration-dependent manner in Ca^{2+}-containing medium. The $[Ca^{2+}]_i$ rise induced by 50 μM *m*-3M3FBS attained to 85 ± 2 nM followed by a plateau. At 1 μM, *m*-3M3FBS did not induce a $[Ca^{2+}]_i$ rise. Fig. 1B shows the concentration-response plot of *m*-3M3FBS-induced $[Ca^{2+}]_i$ response. The Ca^{2+} response saturated at 50 μM *m*-3M3FBS because at a concentration of 60 μM, *m*-3M3FBS did not evoke a different response as that induced by 50 μM. The EC_{50} value was 10 ± 2 μM by using the Hill equation.

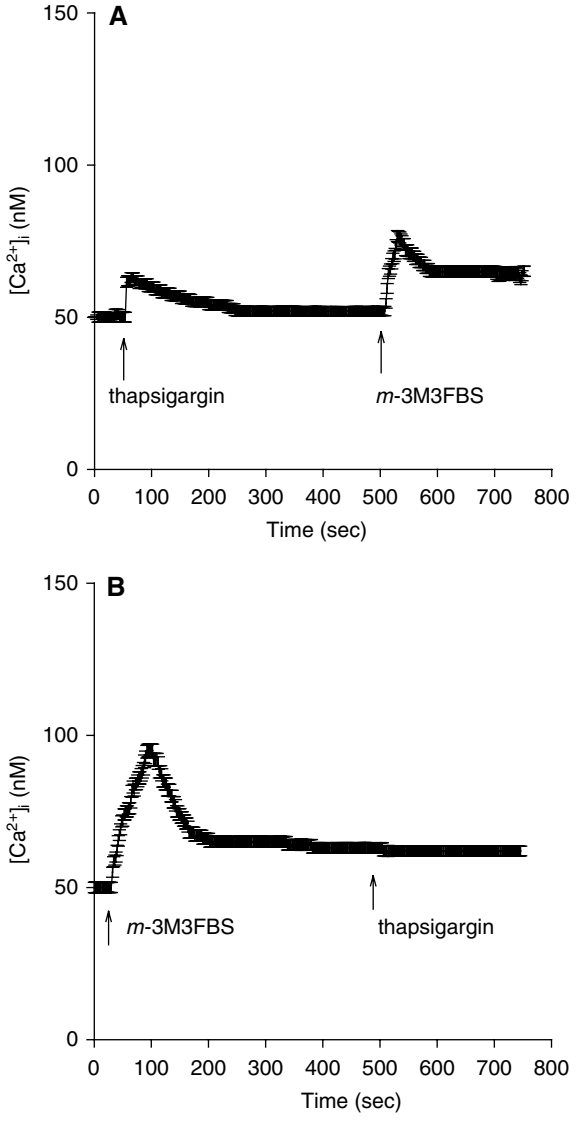

Fig. 3. Intracellular Ca^{2+} stores of *m*-3M3FBS-induced Ca^{2+} release. Experiments were performed in Ca^{2+}-free medium. *M*-3M3FBS (50 μM) and thapsigargin (1 μM) were added at time points indicated. Data are means ± SEM of three experiments.

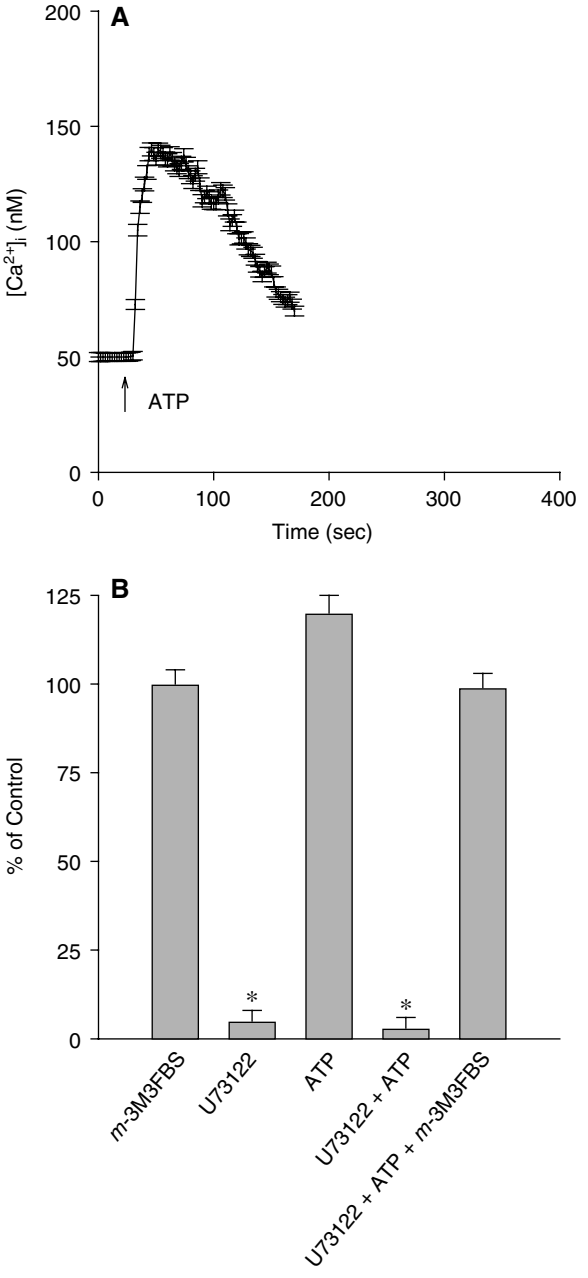

Fig. 4. Lack of effect of U73122 on *m*-3M3FBS-induced Ca^{2+} release. Experiments were performed in Ca^{2+}-free medium. (A) ATP (10 μM) was added as indicated. (B) U73122 (2 μM), ATP (10 μM), and *m*-3M3FBS (50 μM) were added as indicated. Data are means ± SEM of three experiments. *$P < 0.05$ compared to control.

Experiments were performed to explore the Ca^{2+} entry pathway of *m*-3M3FBS-induced response. The store-operated Ca^{2+} influx inhibitors econazole (0.5 μM) and SK&F96365 (1 μM); the Ca^{2+} channel blocker nifedipine (1 μM), GF109230X (2 μM; a protein kinase C (PKC) inhibitor) and aristolochic acid (20 μM; a phospholipase A2 (PLA_2) inhibitor) partly inhibited 50 μM *m*-3M3FBS-induced $[Ca^{2+}]_i$ rise. In contrast, phorbol 12-myristate 13-acetate (PMA; 10 nM; a PKC activator) had no effect on *m*-3M3FBS-induced $[Ca^{2+}]_i$ rise (Fig. 2).

Previous reports have shown that the endoplasmic reticulum is the major Ca^{2+} store in HA59T cells (6, 7). Fig. 3A shows that in Ca^{2+}-free medium, addition of 1 μM thapsigargin, an inhibitor of endoplasmic reticulum Ca^{2+} pumps (30), induced a transient $[Ca^{2+}]_i$ rise of 20 ± 2 nM. *M*-3M3FBS added afterwards induced a $[Ca^{2+}]_i$ rise of 25 ± 2 nM. Conversely, Fig. 3B shows that addition of *m*-3M3FBS (50 μM) induced a $[Ca^{2+}]_i$ rise of 46 ± 2 nM followed by a slow decay. Thapsigargin added at 500 sec failed to induce a $[Ca^{2+}]_i$ rise.

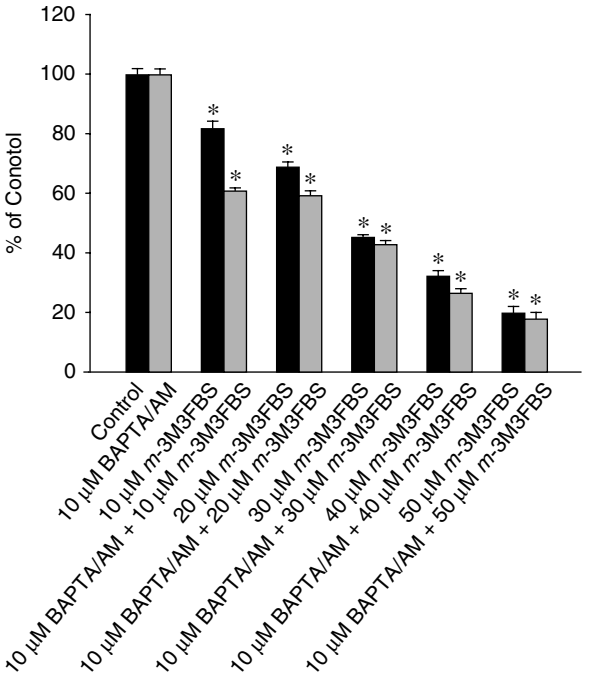

Fig. 5. Cytotoxic effect of *m*-3M3FBS. Cells were treated with 0-50 μM *m*-3M3FBS for 24 h, and the cell viability assay was performed. Data are means ± SEM of three experiments. Each treatment had six replicates (wells). Data are expressed as percentage of control response that is the increase in cell numbers in *m*-3M3FBS-free groups. Control had 10,568 ± 288 cells/well before experiments, and had 13,951 ± 887 cells/well after incubation for 24 h. $*P < 0.05$ compared to control. In each group, the Ca^{2+} chelator BAPTA/AM (10 μM) was added to cells followed by treatment with *m*-3M3FBS in medium. Cell viability assay was subsequently performed. $*P < 0.05$ compared to control.

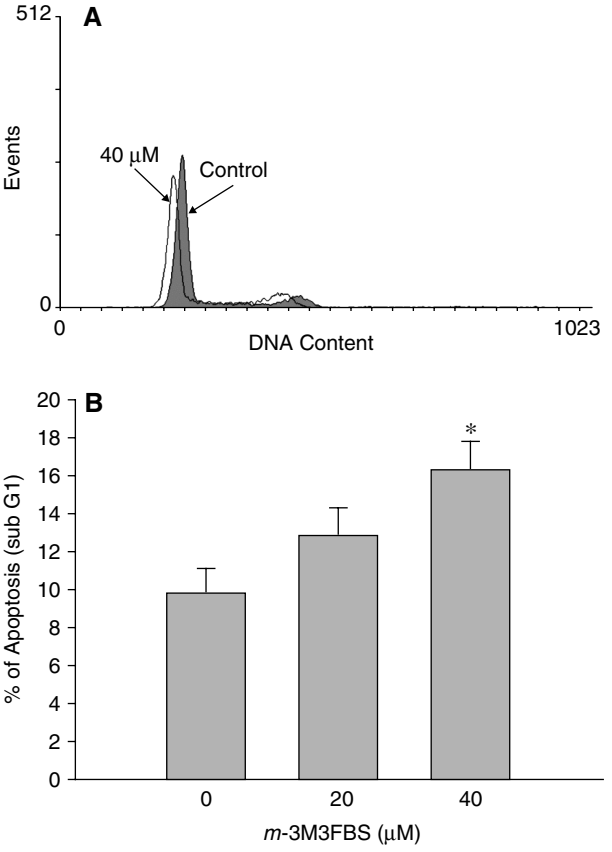

Fig. 6. Effect of *m*-3M3FBS on apoptosis in HA59T cells. Cells were incubated with 20 μM or 40 μM *m*-3M3FBS for 24 h. (A) Attached and floating cells were pooled, treated with PI and analyzed by cytofluorimetry. Typical cell cycle plots are shown: cells undergoing apoptosis are localized in subG1 regions. (B) Percentage of apoptotic cells in subG1 region. N = 3, $*P < 0.05$ compared to control.

PLC-dependent formation of inositol 1,4,5-trisphosphate (IP_3) is a crucial step for releasing Ca^{2+} from the endoplasmic reticulum (4). Because *m*-3M3FBS was able to release Ca^{2+} from the endoplasmic reticulum, the role of IP_3 in this release was explored. U73122, an inhibitor of IP_3 formation (31), was applied to see whether IP_3 was required for *m*-3M3FBS-induced Ca^{2+} release. Fig. 4A shows that ATP (10 μM) induced a $[Ca^{2+}]_i$ rise of 91 ± 2 nM. ATP is an IP_3-dependent agonist of $[Ca^{2+}]_i$ rise in most cell types (14). Fig. 4B shows that incubation with 2 μM U73122 did not change basal $[Ca^{2+}]_i$ but abolished ATP-induced $[Ca^{2+}]_i$ rise. This suggests that U73122 effectively suppressed IP_3 formation. Fig. 4B also shows that addition of 50 μM *m*-3M3FBS after U73122 and ATP treatments caused a $[Ca^{2+}]_i$ rise not different from control.

Given that acute incubation with *m*-3M3FBS induced a substantial $[Ca^{2+}]_i$ rise, and that unregulated $[Ca^{2+}]_i$ rises often alter cell viability (4), experiments were performed to examine the effect of *m*-3M3FBS on viability of HA59T cells. Cells were treated with 0-50 μM *m*-3M3FBS for 24 h, and the tetrazolium assay was performed. In the presence of 10-50 μM *m*-3M3FBS, cell viability decreased in a concentration-dependent manner with an EC_{50} value of 25 ± 1 μM (Fig. 5).

The next question was whether the *m*-3M3FBS-induced cytotoxicity was related to a preceding $[Ca^{2+}]_i$ rise. The intracellular Ca^{2+} chelator BAPTA/AM (10 μM) (33) was used to prevent a $[Ca^{2+}]_i$ rise during *m*-3M3FBS pretreatment. This BAPTA/AM treatment completely inhibited 50 μM *m*-3M3FBS-induced $[Ca^{2+}]_i$ rise (data not shown). Fig. 5 shows that 10 μM BAPTA/AM loading did not alter control cell viability. In the presence of 10-40 μM *m*-3M3FBS, BAPTA/AM loading failed to prevent *m*-3M3FBS-induced cell death (n = 3; $P > 0.05$).

Apoptosis was measured by PI staining of cellular DNA. Fig. 6A shows that the subG1 phase

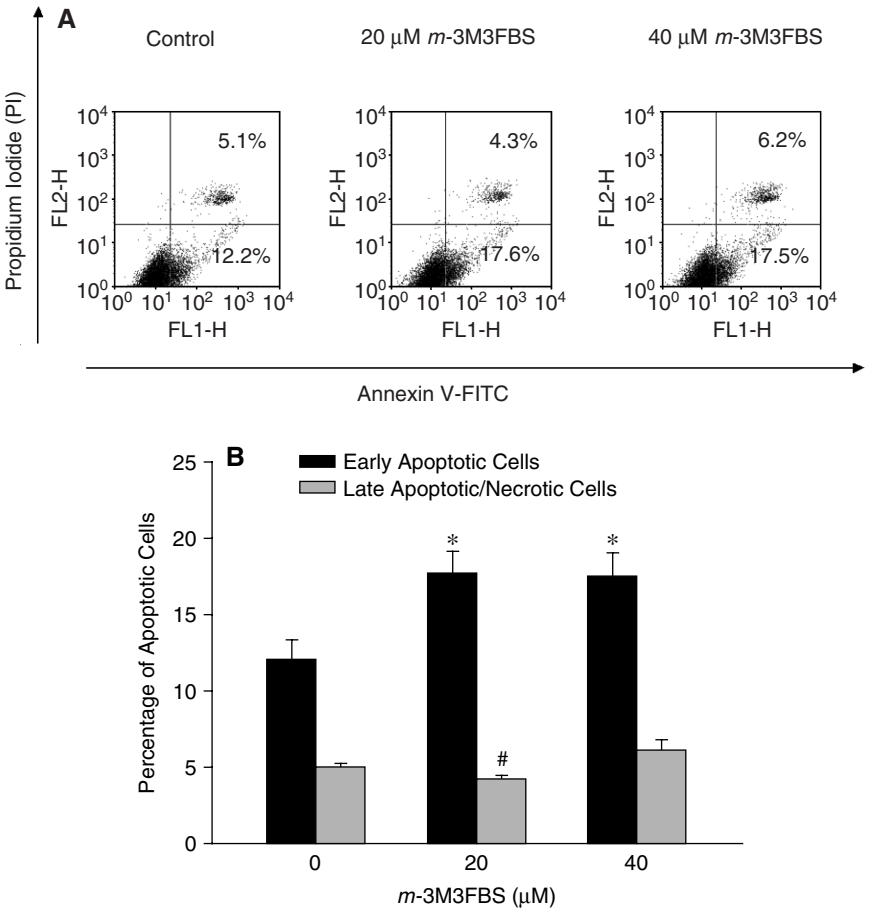

Fig. 7. *M*-3M3FBS-induced apoptosis/necrosis as measured by Annexin V/PI staining. (A) Cells were treated with 0, 20, or 40 μM *m*-3M3FBS, respectively, for 24 h. Cells were then processed for Annexin V/PI staining and analyzed by flow cytometry. (B) The percentage of early apoptotic cells and late apoptotic/necrotic cells. $^{*,\#}P < 0.05$ compared to respective control.

was 9.5 ± 1.3% in control, and after incubation with 40 μM *m*-3M3FBS for 24 h, subG1 phase increased to 16.3 ± 1.5%. This suggests that *m*-3M3FBS induced apoptosis. The extent of *m*-3M3FBS-induced apoptosis was explored and the data are shown in Fig. 6B. At a concentration of 20 μM, *m*-3M3FBS did not cause apoptosis (n = 3; $P > 0.05$). In the presence of 40 μM *m*-3M3FB, 16.3 ± 1.5% of cells were found apoptotic ($P < 0.05$). Annexin V/PI staining was further applied to detect apoptotic/necrotic cells after *m*-3M3FBS treatment. Figs. 7A and B show that treatment with 20 μM or 40 μM *m*-3M3FBS significantly induced apoptosis but not necrosis.

ROS are associated with multiple cellular functions such as cell proliferation, differentiation, and apoptosis (4). To investigate whether *m*-3M3FBS induced oxidative stress in HA59T cells, the levels of intracellular ROS including superoxide anion (O_2^-) and hydrogen peroxide (H_2O_2) in *m*-3M3FBS-treated cells were measured by flow cytometry using DHE and DCFH-DA fluorescent dyes, respectively. It was found that 20 and 40 μM *m*-3M3FBS treatment elevated the intracellular levels of H_2O_2, but not O_2^- (Fig. 8).

Discussion

Our data suggest that *m*-3M3FBS evoked an immediate $[Ca^{2+}]_i$ rise followed by a slow decline phase in Ca^{2+}-containing medium. In contrast, *m*-3M3FBS was shown to induce a spiky $[Ca^{2+}]_i$ rise in neutrophils (1) and a slowly developing $[Ca^{2+}]_i$ rise in SH-SY5Y cells (21). In SH-SY5Y cells, $[Ca^{2+}]_i$ rise was attributed to Ca^{2+} release from stores, whereas our data show that removal of extracellular Ca^{2+} partially reduced the *m*-3M3FBS-induced $[Ca^{2+}]_i$ rise suggesting contribution from both Ca^{2+} entry and Ca^{2+} release. In SH-SY5Y cells, it was shown that U73122 strongly inhibited *m*-3M3FBS-mediated Ca^{2+} release; in contrast, our data show that U73122 did not change *m*-3M3FBS-induced $[Ca^{2+}]_i$ rise. Thus the effects of *m*-3M3FBS on $[Ca^{2+}]_i$ and the underlying pathways may vary among different cell types.

We show that *m*-3M3FBS induced concentra-

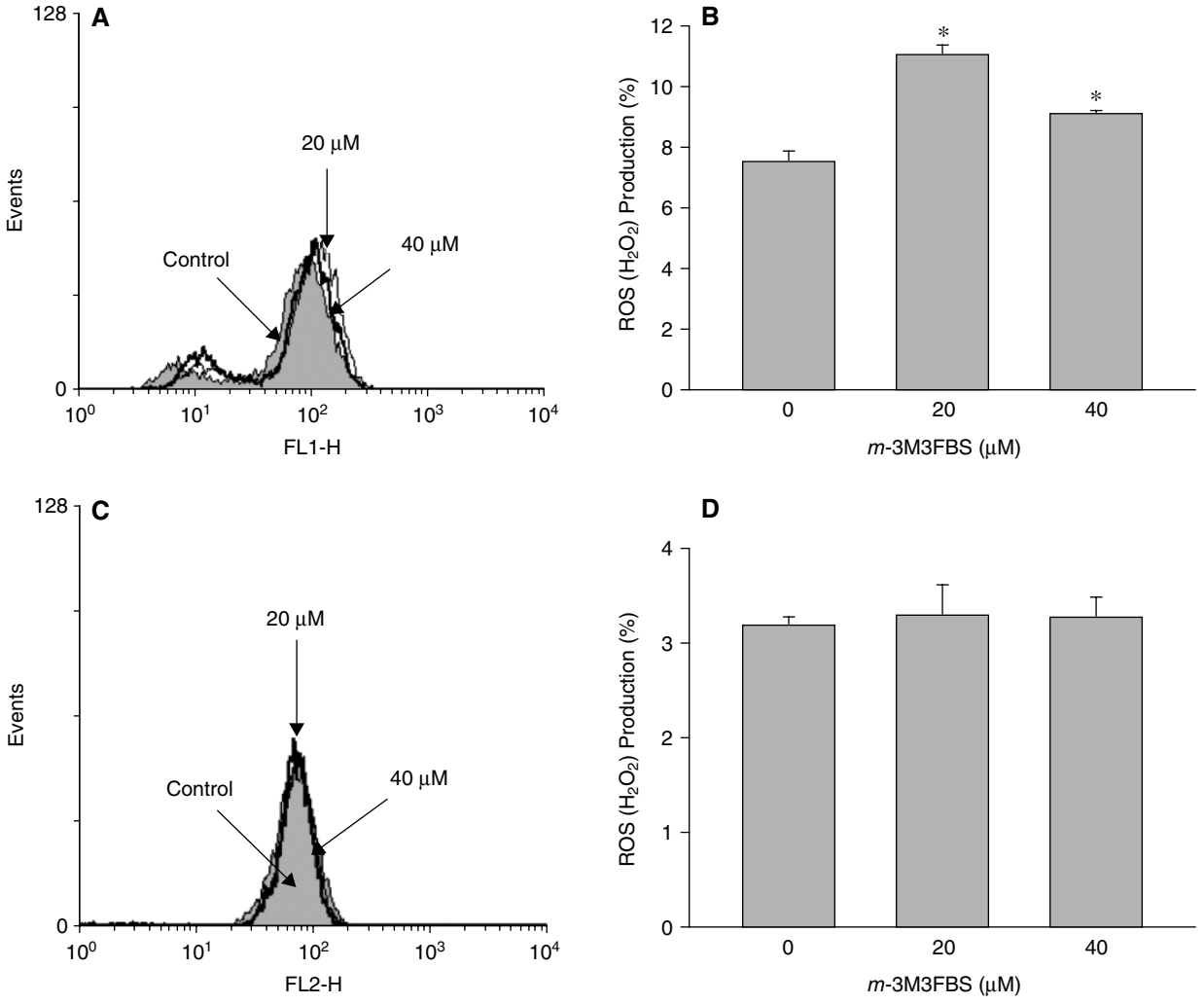

Fig. 8. (A) Effect of *m*-3M3FBS on the hydrogen peroxide level. 2',7'-dichlorofluorescein-diacetate (DCFH-DA) fluorescence was measured after treatment with 0, 20 or 40 μM *m*-3M3FBS in serum-free culture media for 24 h. The fluorescence was quantified using the BD Cell Quest software. Data were means ± SEM of four experiments. $*P < 0.05$ compared to control. (B) Effect of *m*-3M3FBS on the superoxide anion level. Dihydroethidine (DHE) fluorescence in cells was measured after treatment with 0, 20 or 40 μM *m*-3M3FBS in serum-free culture media for 24 h. The fluorescence was quantified using the BD Cell Quest software. Data were means ± SEM of four experiments. The data are represented as DCFH-DA (or DHE) fluorescence percentage that refers to cells positive to DCFH-DA (or DHE). Controls are shown in the first column.

tion-dependent $[Ca^{2+}]_i$ rise in hepatoma cells between 10 μM and 50 μM. Removal of extracellular Ca^{2+} reduced the *m*-3M3FBS-induced response throughout the measurement period, suggesting that Ca^{2+} influx occurred during the whole stimulation period.

The pathways of *m*-3M3FBS-induced Ca^{2+} entry was explored and it was shown that *m*-3M3FBS might evoke Ca^{2+} entry through stimulating store-operated Ca^{2+} entry, a Ca^{2+} influx route induced by depletion of certain Ca^{2+} stores (26). Three Ca^{2+} entry blockers were utilized. Recent evidence shows that nifedipine not only blocks L-type Ca^{2+} channels but also blocks store-operated Ca^{2+} channels (27, 36). Econazole and SK&F96365 are widely used as store-operated Ca^{2+} entry blockers (18, 29). Aristolochic acid is a PLA_2 inhibitor, and was found to inhibit *m*-3M3FBS-induced $[Ca^{2+}]_i$ rise. This suggests that PLA_2 may be involved in *m*-3M3FBS-induced Ca^{2+} movement. Evidence shows that PLA_2 is involved in maintaining endothelial store-operated Ca^{2+} entry and vascular tone in aorta (2), and stimulates store-operated Ca^{2+} entry in dystrophic skeletal muscle fibers (3). Furthermore, because activation of PLC produces IP_3 and diacylglycerol, which activates PKC, the effect of regulation of PKC activity on *m*-3M3FBS-induced $[Ca^{2+}]_i$ rise was examined. Our data show that *m*-3M3FBS-induced $[Ca^{2+}]_i$ rise was decreased by inhibition of PKC activity.

The next question was the Ca^{2+} stores responsible for *m*-3M3FBS-induced Ca^{2+} release. The thapsi-

gargin-sensitive endoplasmic reticulum stores appear to be the main stores because thapsigargin pretreatment reduced a major part of *m*-3M3FBS-induced $[Ca^{2+}]_i$ rise; and conversely, pretreatment with *m*-3M3FBS abolished thapsigargin-induced $[Ca^{2+}]_i$ rise. Since thapsigargin did not abolish *m*-3M3FBS-induced Ca^{2+} release, the role of other Ca^{2+} stores might be explored. These include NAADP- (5) or cADP-ribose-dependent (15) stores since they are partially insensitive to thapsigargin. Furthermore, *m*-3M3FB also may inhibit secretory pathway Ca^{2+} ATPases (SPCAs) (34, 35).

Although *m*-3M3FBS mainly release Ca^{2+} from endoplasmic reticulum, it seems that IP_3-dependent pathways did not play a role in the Ca^{2+} release, since the response was not changed when IP_3 production was inhibited by U73122. In SH-SY5Y cells, 25 μM *m*-3MFBS was shown to fail to activate PLC and did not stimulate inositol phosphate generation (21). *M*-3M3FBS might release Ca^{2+} similarly to thapsigargin by inhibiting endoplasmic reticulum Ca^{2+} pumps.

M-3M3FBS was found to be cytotoxic to hepatoma cells in a concentration-dependent manner. Because *m*-3M3FBS induced a $[Ca^{2+}]_i$ rise and cell death, it would be interesting to know whether the death resulted from the Ca^{2+} overloading. Our data show that the *m*-3M3FBS-induced cell death was not reversed when cytosolic Ca^{2+} was chelated. This implies that *m*-3M3FBS-induced cell death was independent of a $[Ca^{2+}]_i$ rise. Furthermore, cell cycle analysis and Annexin/PI staining data suggest that *m*-3M3FBS-induced cell death involved apoptosis, which is consistent with the apoptotic effect of *m*-3M3FBS observed in other cell lines. In contrast, *m*-3M3FBS was shown to induce apoptosis that was attenuated by chelating intracellular Ca^{2+} in human renal Caki cancer cells (20). Lee *et al*. (22) showed that *m*-3M3FBS induced a $[Ca^{2+}]_i$ rise in monocytic leukemia cell leading to apoptosis. It is known that apoptosis consists of external and internal pathways. Thus, the role of mitochondria in *m*-3M3FBS-induced apoptosis was explored by measuring ROS levels. Our data suggest that *m*-3M3FBS at concentrations that induced $[Ca^{2+}]_i$ rises also induced H_2O_2 production. Thus it is likely that ROS production is involved in *m*-3M3FBS-induced apoptosis. This is the first report that *m*-3M3FBS induced H_2O_2 production in any cell type. Our data show an apparent contradiction between experiments of viability and apoptosis/necrosis. Viability had a reduction to about 70% with 20 μM *m*-3M3FBS and to about 30-35% with 40 μM *m*-3M3FBS. On the contrary, at both concentrations apoptosis had a very modest increase, and no increase in late apoptotic/necrotic cells was observed. This could be due to a mitochondrial dysfunction not accompanied by cellular death.

Together, the data show that *m*-3M3FBS induced Ca^{2+} release from endoplasmic reticulum in a PLC-independent manner and also caused Ca^{2+} influx *via* PLA_2-, PKC-dependent store-operated Ca^{2+} entry pathway. *M*-3M3FBS also evoked cell death *via* Ca^{2+}-dissociated apoptotic pathways involving H_2O_2 production. Caution should be applied in using 25 μM *m*-3M3FBS as a putative PLC activator, given its ability to elevate $[Ca^{2+}]_i$ and to induce oxidation-mediated apoptosis. Because a $[Ca^{2+}]_i$ rise can interfere with numerous cellular processes such as secretion, gene expression, protein synthesis, contraction, viability, *etc.*, previous studies that used *m*-3M3FBS as a presumed PLC activator might have reported data resulted from effects induced by $[Ca^{2+}]_i$ rise and cytotoxicty, instead of PLC activation. The present study might help avoid these errors associated with Ca^{2+} and cytotoxicy.

Acknowledgments

This work was supported by a grant from Kaohsiung Veterans General Hospital (VGHKS100-102) to CR Jan.

References

1. Bae, Y.S., Lee, T.G., Park, J.C., Hur, J.H., Kim, Y., Heo, K., Kwak, J.Y., Suh, P.G. and Ryu, S.H. Identification of a compound that directly stimulates phospholipase C activity. *Mol. Pharmacol*. 63: 1043-1050, 2003.
2. Boittin, F.X., Gribi, F., Serir, K. and Bény, J.L. Ca^{2+}-independent PLA2 controls endothelial store-operated Ca^{2+} entry and vascular tone in intact aorta. *Am. J. Physiol. Heart Cir. Physiol*. 295: H2466-H2474, 2008.
3. Boittin, F.X., Petermann, O., Hirn Mittaud, P., Dorchies, O.M., Roulet, E. and Ruegg, U.T. Ca^{2+}-independent phospholipase A_2 enhances store-operated Ca^{2+} entry in dystrophic skeletal muscle fibers. *J. Cell Sci*. 119: 3733-3742, 2006.
4. Bootman, M.D., Berridge, M.J. and Roderick, H.L. Calcium signalling: more messengers, more channels, more complexity. *Cur. Biol*. 12: R563-R565, 2002.
5. Calcraft, P.J., Ruas, M., Pan, Z., Cheng, X., Arredouani, A., Hao, X., Tang, J., Rietdorf, K., Teboul, L., Chuang, K.T., Lin, P., Xiao, R., Wang, C., Zhu, Y., Lin, Y., Wyatt, C.N., Parrington, J., Ma, J., Evans, A.M., Galione, A. and Zhu, M.X. NAADP mobilizes calcium from acidic organelles through two-pore channels. *Nature* 459: 596-600, 2009.
6. Chang, K.H., Tan, H.P., Kuo, C.C., Kuo, D.H., Shieh, P., Chen, F.A. and Jan, C.R. Effect of nortriptyline on Ca^{2+} handling in SIRC rabbit corneal epithelial cells. *Chinese J. Physiol* 53: 178-184, 2010.
7. Cheng, J.S., Huang, C.C., Chou, C.T. and Jan, C.R. Mechanisms of carvedilol-induced $[Ca^{2+}]_i$ rises and death in human hepatoma cells. *Naunyn Schmiedebergs Arch. Pharmacol*. 376: 185-194, 2007.
8. Cheng, J.S., Shu, S.S., Kuo, C.C., Chou, C.T., Tsai, W.L., Fang, Y.C., Kuo, L.N., Yeh, J.H., Chen, W.C., Chien, J.M., Lu, T., Pan, C.C., Cheng, H.H., Chai, K.L. and Jan, C.R. Effect of diindolylmethane on $[Ca^{2+}]_i$ movement and viability in HA59T human hepatoma cells. *Arch. Toxicol.* 85: 1257-1266, 2011.
9. Clapham, D.E. Intracellular calcium. Replenishing the stores. *Nature* 375: 634-635, 1995.

10. Clapp, T.R., Medler, K.F., Damak, S., Margolskee, R.F. and Kinnamon, S.C. Mouse taste cells with G protein-coupled taste receptors lack voltage-gated calcium channels and SNAP-25. *BMC Biol*. 4: 7, 2006.
11. Díaz Añel, A.M. Phospholipase C β3 is a key component in the Gβγ/PKCε/PKD-mediated regulation of *trans*-Golgi network to plasma membrane transport. *Biochem. J*. 406: 157-165, 2007.
12. Fang, Y.C., Chou, C.T., Pan, C.C., Hsieh, Y.D., Liang, W.Z., Chao, D., Tsai, J.Y., Liao, W.C., Kuo, D.H., Shieh, P., Kuo, C.C., Jan, C.R. and Shaw, C.F. Paroxetine-induced Ca^{2+} movement and death in OC2 human oral cancer cells. *Chinese J. Physiol*. 54: 310-317, 2011.
13. Fang, Y.C., Kuo, D.H., Shieh, P., Chen, F.A., Kuo, C.C. and Jan, C.R. Effect of *m*-3M3FBS on Ca^{2+} movement in Madin-Darby canine renal tubular cells. *Human Exp. Toxicol*. 28: 655-663, 2009.
14. Florenzano, F., Viscomi, M.T., Mercaldo, V., Longone, P., Bernardi, G., Bagni, C., Molinari, M. and Carrive, P. P2X2R purinergic receptor subunit mRNA and protein are expressed by all hypothalamic hypocretin/orexin neurons. *J. Com. Neurol*. 498: 58-67, 2006.
15. Gerasimenko, J.V., Sherwood, M., Tepikin, A.V., Petersen, O.H. and Gerasimenko, O.V. NAADP, cADPR and IP3 all release Ca^{2+} from the endoplasmic reticulum and an acidic store in the secretory granule area. *J. Cell Sci*. 119: 226-238, 2006.
16. Grynkiewicz, G., Poenie, M. and Tsien, R.Y. A new generation of Ca^{2+} indicators with greatly improved fluorescence properties. *J. Biol. Chem*. 260: 3440-3450, 1985.
17. Hattori, T. and Wang, P.L. Calcium antagonists cause dry mouth by inhibiting resting saliva secretion. *Life Sci*. 81: 683-690, 2007.
18. Ishikawa, J., Ohga, K., Yoshino, T., Takezawa, R., Ichikawa, A., Kubota, H. and Yamada, T. A pyrazole derivative, YM-58483, potently inhibits store-operated sustained Ca^{2+} influx and IL-2 production in T lymphocytes. *J. Immunol*. 170: 4441-4449, 2003.
19. Jajoo, S., Mukherjea, D., Brewer, G.J. and Ramkumar, V. Pertussis toxin B-oligomer suppresses human immunodeficiency virus-1 Tat-induced neuronal apoptosis through feedback inhibition of phospholipase C-β by protein kinase C. *Neuroscience* 151: 525-532, 2004.
20. Jung, E.M., Lee, T.J., Park, J.W., Bae, Y.S., Kim, S.H., Choi, Y.H. and Kwon, T.K. The novel phospholipase C activator, *m*-3M3FBS, induces apoptosis in tumor cells through caspase activation, down-regulation of XIAP and intracellular calcium signaling. *Apoptosis* 13: 133-145, 2008.
21. Krjukova, J., Holmqvist, T., Danis, A.S., Akerman, K.E. and Kukkonen, J.P. Phospholipase C activator *m*-3M3FBS affects Ca^{2+} homeostasis independently of phospholipase C activation. *Brit. J. Pharmacol*. 143: 3-7, 2004.
22. Lee, Y.N., Lee, H.Y., Kim, J.S., Park, C., Choi, Y.H., Lee, T.G., Ryu, S.H., Kwak, J.Y. and Bae, Y.S. The novel phospholipase C activator, *m*-3M3FBS, induces monocytic leukemia cell apoptosis. *Cancer Lett*. 222: 227-235, 2005.
23. Liao, W.C., Huang, C.C., Cheng, H.H., Wang, J.L., Lin, K.L., Cheng, J.S., Chai, K.L., Hsu, P.T., Tsai, J.Y., Fang, Y.C., Lu, Y.C., Chang, H.T., Huang, J.K., Chou, C.T. and Jan, C.R. Effect of calmidazolium on $[Ca^{2+}]_i$ and viability in human hepatoma cells. *Arch. Toxicol*. 83: 61-68, 2009.
24. Lin, C.H., Liu, M.C., Lin, M.S., Lin, P.L., Chen, Y.H., Chen, C.T., Chen, I.M. and Tsai, M.C. Effects of a new isoquinolinone derivative on induction of action potential bursts in central snail neuron. *Pharmacology* 75: 98-110, 2005.
25. Nam, J.H., Lee, H.S., Nguyen, Y.H., Kang, T.M., Lee, S.W., Kim, H.Y., Kim, S.J., Earm, Y.E. and Kim, S.J. Mechanosensitive activation of K^+ channel *via* phospholipase C-induced depletion of phosphatidylinositol 4,5-bisphosphate in B lymphocytes. *J. Physiol*. 582: 977-990, 2007.
26. Putney, J.W. Jr. A model for receptor-regulated calcium entry. *Cell Calcium* 7: 1-12, 1986.
27. Quinn, T., Molloy, M., Smyth, A. and Baird, A.W. Capacitative calcium entry in guinea pig gallbladder smooth muscle *in vitro*. *Life Sci*. 74: 1659-1669, 2004.
28. Rao, J.N., Liu, L., Zou, T., Marasa, B.S., Boneva, D., Wang, S.R., Malone, D.L., Turner, D.J. and Wang, J.Y. Polyamines are required for phospholipase C-γ expression promoting intestinal epithelial restitution after wounding. *Am. J. Physiol. Gastrointestinal Liver Physiol*. 292: G335-G343, 2007.
29. Shideman, C.R., Reinardy, J.L. and Thayer, S.A. Gamma-Secretase activity modulates store-operated Ca^{2+} entry into rat sensory neurons. *Neurosci. Lett*. 451: 124-128, 2009.
30. Thastrup, O., Cullen, P.J., Drøbak, B.K., Hanley, M.R. and Dawson, A.P. Thapsigargin, a tumor promoter, discharges intracellular Ca^{2+} stores by specific inhibition of the endoplasmic reticulum Ca^{2+}-ATPase. *Proc. Natl. Acad. Sci. USA* 87: 2466-2470, 1990.
31. Thompson, A.K., Mostafapour, S.P., Denlinger, L.C., Bleasdale, J.E. and Fisher, S.K. The aminosteroid U-73122 inhibits muscarinic receptor sequestration and phosphoinositide hydrolysis in SK-N-SH neuroblastoma cells. A role for Gp in receptor compartmentation. *J. Biol. Chem*. 266: 23856-23862, 1991.
32. Tsai, J.Y., Shieh, P., Kuo, D.H., Chen, F.A., Kuo, C.C. and Jan, C.R. Effect of *m*-3M3FBS on Ca^{2+} movement in PC3 human prostate cancer cells. *Chinese J. Physiol*. 53: 151-159, 2010.
33. Tsien, R.Y. New calcium indicators and buffers with high selectivity against magnesium and protons: design, synthesis, and properties of prototype structures. *Biochemistry* 19: 2396-2404, 1980.
34. Wuytack, F., Raeymaekers, L. and Missiaen, L. Molecular physiology of the SERCA and SPCA pumps. *Cell Calcium* 32: 279-305, 2002.
35. Wuytack, F., Raeymaekers, L. and Missiaen, L. PMR1/SPCA Ca^{2+} pumps and the role of the Golgi apparatus as a Ca^{2+} store. *Pflugers Arch*. 446: 148-153, 2003.
36. Young, R.C., Schumann, R. and Zhang, P. Nifedipine block of capacitative calcium entry in cultured human uterine smooth-muscle cells. *J. Soc. Gynecol. Invest*. 8: 210-215, 2001.